



**HAL**  
open science

## Time-concentration profiles of tire particle additives and transformation products under natural and artificial aging

Loélia Fohet, Jean-Michel Andanson, Tiffany Charbouillot, Lucie Malosse, Martin Lereboure, Florence Delor-Jestin, Vincent Verney

### ► To cite this version:

Loélia Fohet, Jean-Michel Andanson, Tiffany Charbouillot, Lucie Malosse, Martin Lereboure, et al.. Time-concentration profiles of tire particle additives and transformation products under natural and artificial aging. Science of the Total Environment, 2023, 859, pp.160150. 10.1016/j.scitotenv.2022.160150 . hal-04236618

HAL Id: hal-04236618

<https://hal.science/hal-04236618v1>

Submitted on 11 Oct 2023

**HAL** is a multi-disciplinary open access archive for the deposit and dissemination of scientific research documents, whether they are published or not. The documents may come from teaching and research institutions in France or abroad, or from public or private research centers.

L'archive ouverte pluridisciplinaire **HAL**, est destinée au dépôt et à la diffusion de documents scientifiques de niveau recherche, publiés ou non, émanant des établissements d'enseignement et de recherche français ou étrangers, des laboratoires publics ou privés.



Distributed under a Creative Commons Attribution - NonCommercial - ShareAlike 4.0 International License

1 **Title: Time-concentration profiles of tire particle additives and transformation products under natural**  
2 **and artificial aging**

3 **Authors:** Loélia Fohet<sup>1,2</sup>, Jean-Michel Andanson<sup>1</sup>, Tiffany Charbouillot<sup>2</sup>, Lucie Malosse<sup>2</sup>, Martin  
4 Leremboure<sup>1</sup>, Florence Delor-Jestin\*<sup>1</sup>, Vincent Verney<sup>1</sup>

5 <sup>1</sup> Université Clermont Auvergne, Clermont Auvergne INP, CNRS, ICCF, F-63000 Clermont-Ferrand, France

6 <sup>2</sup> Manufacture Française des Pneumatiques MICHELIN, Centre de Technologies Ladoux, 63040 Clermont-  
7 Ferrand, France

8 \* Corresponding author: [florence.delor\\_jestin@sigma-clermont.fr](mailto:florence.delor_jestin@sigma-clermont.fr)

9  
10 **Abstract:** Tire and road wear particles (TRWP) are polymer-based microparticles that are emitted into  
11 the environment during tire usage. Growing efforts are currently being made to quantify these  
12 emissions, characterize the leachates and assess their environmental impact. This study aimed to  
13 investigate the effect of aging on TRWP composition. Cryomilled tire tread particles (CMTTP) and TRWP  
14 were exposed for different durations to three aging conditions: accelerated thermal and photochemical  
15 aging and natural outdoor aging. Particles were then extracted with cyclohexane/ethanol. The time-  
16 concentration profiles of 23 additives and transformation products present in these extracts were  
17 determined by UHPLC-HRMS. Several chemicals, such as N-(1,3-dimethylbutyl)-N'-phenyl-p-  
18 phenylenediamine (6-PPD) or 1,3-diphenylguanidine (DPG), decayed exponentially under all aging  
19 conditions, with half-lives of a few days under artificial photoaging versus dozens of days under pure  
20 thermal aging at 60 °C. The natural aging profiles lie between those 2 laboratory aging conditions. Other  
21 chemicals, such as 6PPD-quinone, presented bell-shaped concentration profiles within CMTTP when  
22 particles were exposed to UV light. 6PPD-quinone reached a maximal concentration within a month  
23 under natural aging. For TRWP, the initial load of 6PPD-quinone had already reached a maximum prior to  
24 the aging experiments and decreased exponentially under natural aging with a half-life below one  
25 month. Pure thermal aging induced a significantly slower decay of 6PPD-quinone within TRWP (half-life  
26 of half a year), emphasizing a greater stability and persistence in environmental compartments without  
27 light. This study highlighted that the more readily accessible CMTTP could be considered a reasonable  
28 proxy of TRWP to investigate the fate of chemicals within rubber particles, at least from a qualitative  
29 standpoint. Overall, the concentrations of 20 of the evaluated chemicals decreased by more than 50%  
30 within 50 days under natural aging.

31  
32 **Highlights:**

- 33 - Time-concentration profiles of 23 chemicals were determined for 3 types of aging  
34 - Transformation products showed different aging-induced concentration profiles  
35 - Concentrations of most chemicals were halved within 50 days under natural aging  
36 - The 6PPD-quinone half-life in TRWP was within a month when exposed to natural light  
37 - Cryomilled tire tread particles can be used as TRWP surrogates to assess aging

38 **Keywords:** Tire and road wear particles (TRWP), aging, UHPLC-HRMS, N,N'-diphenylguanidine (DPG), N-  
39 (1,3-dimethylbutyl)-N'-phenyl-p-phenylenediamine (6PPD), 6PPD-quinone

## 40 **Abbreviations:**

- 41 6QDI: N-Phenyl-N'-1,3-dimethylbutyl-p-quinonediimine (CAS: 52870-46-9)  
42 6PPD: N-(1,3-dimethylbutyl)-N'-phenyl-p-phenylenediamine (CAS: 793-24-8)  
43 6PPD-quinone: 2-anilino-5-[(4-methylpentan-2-yl)amino]-cyclohexa-2,5-diene-1,4-dione  
44 BR: Butadiene Rubber  
45 BT: benzothiazole (CAS: 95-16-9)  
46 CBS: N-cyclohexylbenzothiazole-2-sulfenamide (CAS: 95-33-0)  
47 CMTTP: Cryomilled tire tread particles  
48 DPG: 1,3-diphenylguanidine (CAS: 102-06-7)  
49 DT50: Dissipation time at 50%, the time required for the concentration to reach half of the initial value  
50 ESI: Electrospray ionization  
51 NR: Natural Rubber  
52 PM2.5: particulate matter with a diameter less than 2.5  $\mu\text{m}$   
53 PM10: particulate matter of diameter less than 10  $\mu\text{m}$   
54 RT: retention time  
55 SBR: Styrene Butadiene Rubber  
56 TMQ: poly(1,2-dihydro-2,2,4-trimethylquinoline) (CAS: 26780-96-1)  
57 TRWP: Tire and road wear particles  
58 UHPLC-HRMS: Ultra-High Performance Liquid Chromatography (UHPLC) coupled with High Resolution  
59 Mass Spectrometry (HRMS)

60

## 61 **1) Introduction**

62 Tire and road wear particle (TRWP) emissions result from the friction of the tread band rubber surface  
63 with the road during the tire rolling usage phase<sup>1</sup>. The resulting particles consist of damaged rubber<sup>2</sup>  
64 with exogenous mineral incrustations derived from road pavement or other sources<sup>3</sup>. Predictions of the  
65 quantity of tire wear released every year were first calculated in the 1970s<sup>4</sup> and it is now roughly  
66 estimated that the order of magnitude of tread wear is approximately 0.1 g/km per car, accounting for a  
67 weight loss of 1 to 1.5 kg over a lifespan of 50 000 km for one tire<sup>1,5-7</sup>. The total amount of tire tread  
68 wear released every year is thus predicted to be close to 6 million tons worldwide<sup>8</sup>. This significant  
69 amount makes TRWP an important topic when assessing the environmental impacts of tires, considering  
70 that after their release, they are transported to different environmental compartments<sup>8-11</sup>. A transport  
71 model approach applied to the Seine watershed recently showed that roadside soil would be the major  
72 sink of TRWP, while 18% of the release would be transported to freshwater and 2% could reach the  
73 estuary<sup>12,13</sup>. Small TRWP can also be released into the air<sup>14-16</sup>. Within each compartment, tire particles  
74 might be subjected to various types of aging and degradation due to exposure to solar radiation,  
75 temperature, rainwater<sup>10,11</sup> and/or microorganisms<sup>10,11</sup>. Investigations of the environmental fate and  
76 health aspects of TRWP were reviewed, and further research is needed with degradation assessment  
77 during long-term monitoring<sup>10</sup>. Photoaging and microbial degradation are considered the most  
78 important aging processes of TRWP<sup>10,17</sup>. Several research efforts have been reported on the aging of  
79 vulcanized rubbers to understand its impact on mechanical properties or tire performance<sup>18,19</sup>. Similarly,  
80 poly(cis-1,4-isoprene) elastomer biodegradation has been largely investigated over the last twenty years  
81 for rubber waste management purposes and biotechnical solution development<sup>20</sup>. Nevertheless, detailed  
82 knowledge of the degradation of TRWP is quite limited<sup>17</sup>.

83 The chemical composition of tire tread is complex. Approximately 30 to 60 wt% of the tire tread is  
84 elastomer material, typically in the form of styrene butadiene rubber (SBR), butadiene rubber (BR) or  
85 natural rubber (NR). Inert fillers, such as carbon black and silica, make up 25 to 35 wt% of the tire tread,  
86 and the remaining mass is a mix of plasticizers, oils, vulcanization agents and protective molecules.<sup>1,21,22</sup>  
87 Approximately 1 to 3 wt% of the tire tread consists of protective molecules (e.g., 6PPD, TMQ), and 1 to 4  
88 wt% is attributed to vulcanization components (e.g., DPG, CBS)<sup>1,22,23</sup>. The manufacturing process and  
89 service life of tires<sup>17</sup> also lead to the formation of transformation products. For example, benzothiazole  
90 (BT) is one of the decomposition products of vulcanization accelerators that are present in tire treads  
91 immediately after the process<sup>24</sup>. Müller *et al.*<sup>25</sup> and Seiwert *et al.*<sup>26</sup> recently evaluated over a hundred  
92 chemicals found in tire leachates that consisted of transformation products of initial tire tread additives.  
93 Consequently, TRWP turned out to be a cocktail of hundreds of chemicals. This important number of  
94 molecules has been an emerging topic since the 1990s<sup>27-29</sup> and has received accelerating interest in the  
95 last two years after the work by Tian *et al.*<sup>30,31</sup> revealed that the transformation product 6PPD-quinone in  
96 tire leachates induces acute toxicity in Coho salmon. The discovery of this molecule raises concerns  
97 about the potential toxicity of tire leachates, especially due to the degradation products that could have  
98 different toxicity and persistence than the parent molecule. In this context, leaching studies from TRWP  
99 or tire cryogrinds have been receiving growing attention and have focused on various substances,  
100 including heavy metals and organic additives<sup>17,25,26,32-34</sup>. Collection and analysis of environmental  
101 samples also revealed the occurrence of several PPD-derived quinones in urban runoff, roadside soils,  
102 and air particles<sup>14</sup>.

103 Degradation of rubber additives can first occur during the tire production stage and usage phase and  
104 continue throughout tire particle lifespan, either *via* abiotic degradation pathways, such as thermo-  
105 oxidation and photooxidation, or sometimes *via* microbial degradation<sup>17</sup>.

106 TMQ and 6PPD are primarily reactive with UV light, oxygen and/or ozone<sup>35</sup>. These molecules migrate  
107 toward the surface of rubber and form a protective film<sup>35-37</sup> that reacts with free radicals and then forms  
108 stable molecules, thereby protecting the elastomer from ozonation and photolysis<sup>35,37-39</sup>. It is therefore  
109 expected that their degradation rapidly occurs during photoaging. The degradation pathways of 6PPD  
110 have previously been documented in the literature<sup>26,34,36</sup> and Seiwert *et al.*<sup>26</sup> identified 38 transformation  
111 products from 6PPD. 6QDI and 6PPD-quinone<sup>30</sup> are two well-known degradation products from 6PPD.  
112 6QDI was described in the 1990s<sup>35,40-42</sup> and is present immediately after 6PPD's first interference with  
113 ozone<sup>26</sup>. Moreover, 6QDI is also sometimes used as an additional antioxidant<sup>40</sup> because it has the  
114 particularity to bind to the elastomer, giving a more efficient protective effect on the elastomer<sup>35</sup>. 6PPD-  
115 quinone was described more recently by Tian *et al.*<sup>30,31,43</sup> but was probably already evidenced in 1983 in  
116 6PPD ozonation experiments carried out by Lattimer *et al.*<sup>36</sup>, who proposed the structure of the dinitrone  
117 isomer at that time. Recent studies on tire particle leachates in water runoff demonstrate the presence  
118 of 6PPD-quinone in the environment<sup>15,25,26,44,45</sup>. On the other hand, DPG degradation products are less  
119 known than 6PPD degradation products. Recently, Müller *et al.*<sup>25</sup> identified 13 possible degradation  
120 products from DPG.

121 However, studies on the thermal and photochemical degradation of tire particles are still rare. In 1980,  
122 Cadle and Williams<sup>46</sup> investigated the degradation of tire wear particles exposed to natural elements  
123 within either roadside soil or glass beads. The remaining elastomer fraction was quantified over time by  
124 pyrolysis-gas chromatography, and the authors estimated a half-life of the polymer in soil of 16 months,  
125 with a significant abiotic contribution. Klöckner *et al.*<sup>34</sup> investigated the accelerated degradation of

126 additives in tire particles after 72 hours of aging under UV light and 20-day aging at 80 °C, while Unice *et*  
127 *al.*<sup>32</sup> and Thomas *et al.*<sup>33</sup> proposed artificial UV light aging of 1 month equivalent to natural aging of 1  
128 year. Klockner *et al.*<sup>34</sup> have identified three potential organic markers to evaluate the presence of TRWP  
129 in sediment and soil (i.e., 6-PPD-quinone, *N*-formyl-6-PPD and hydroxylated *N*-1,3-dimethylbutyl-*N*-  
130 phenyl quinone diimine). Nevertheless, the kinetics of degradation of tire tread additives under  
131 accelerated aging (thermal and photochemical) and under natural weathering conditions are not yet well  
132 known, and there is a lack of knowledge regarding their degradation within tire wear particles.

133 In the present study, a composition analysis was developed, and the amounts of organic chemicals in tire  
134 particles were evaluated prior to and after their aging either under accelerated or natural conditions.  
135 After various times of thermo and/or photoaging of particles, chemicals were extracted from cryomilled  
136 tire tread particles (CMTTP) and from tire and road wear particles (TRWP) with a mixture of  
137 cyclohexane/ethanol, and then chemicals were identified using UHPLC-HRMS. The mixture of  
138 apolar/polar solvents can efficiently extract a wide range of molecules and was thus used to estimate  
139 their fate under various exposures. However, this does not represent real environmental conditions. To  
140 do so, a comparison with water extraction was also proposed. Analyses focused on both tire additives,  
141 such as DPG and 6PPD, and on their transformation products, which were compared to those previously  
142 reported in the literature. This study allowed us to compare the kinetics of both the dissipation of parent  
143 molecules and the formation of intermediate degradation products. The results obtained with CMTTP  
144 under thermo and photoaccelerated aging are presented first and then compared to those obtained  
145 under natural weathering conditions and finally to a similar series of experiments conducted with TRWP.

## 146 **2) Materials and methods**

### 147 **2.1) Materials**

#### 148 **2.1.1) Cryomilled tire tread particles (CMTTP)**

149 Cryogenically milled tire tread particles (CMTTP) of size 0-60 mesh were provided by Michelin company  
150 from a batch produced in 2016. They were obtained from an assembly of several nonworn truck tire  
151 retreading bands (i.e., that never experienced any on-road solicitations). The tire treads were first  
152 ambient ground down to 2-3 cm chips using industrial scissors. Then, the rubber pieces were cooled  
153 using liquid nitrogen to make them brittle before entering a mill where they were shattered into a fine  
154 powder, which was finally sieved to obtain a specific size distribution. Particles were stored protected  
155 from the light at room temperature (20-25 °C) for 2 years after being provided by Michelin in July 2020.  
156 The particle size distribution was characterized via laser diffraction analysis (figure SI 1). Most particles  
157 were between 50 and 300 µm, similar to TRWP. Technical details are described in Section 2.4.1.

158

#### 159 **2.1.2) Tire and road wear particles (TRWP) on-road driving collection system**

160 Michelin Engineering Services developed and designed an on-road driving collection device<sup>47</sup> for a rear-  
161 wheel-drive passenger car (BMW 530i, 2001) to collect TRWP and to capture PM10 and PM2.5. This  
162 device was positioned close to the rear left wheel, as the right side of roads is more contaminated with  
163 external pollution (i.e., vegetation, minerals, ...) than the left side. This device was composed of three  
164 nozzles attached to the brake caliper and connected to three vacuums (Easy-Clean 200, Aspilusa, 1400 W

165 each), which were located within a trailer attached to the car. The collection system was powered using  
166 a power generating unit (GYW-9 M5, Genelec, 230 V, 6000 W) located within the trailer.

167 The nozzles (Figure SI 2) were designed by Eric Centre SAS (Riom, France) and produced by 3D printing.  
168 The shape of the nozzles was optimized to avoid air turbulence and to maximize the air flow. To ensure  
169 that the collection system was not clogged during the test, the velocity of the air flow was systematically  
170 measured before and after each test at the entrance of each nozzle, and the drift did not exceed 5%. The  
171 air flow rate measured at the entrance of each nozzle was  $75 \pm 5 \text{ m}^3/\text{h}$ .

172 TRWP were collected in 2019 from a summer tire (Michelin Primacy 4, 225/45 R17 91 W, which was  
173 manufactured the same year and had already experienced a few hundreds of km of service prior to the  
174 TRWP collection step) on the high-speed track (Figure SI 3) on the Michelin test center of Ladoux, near  
175 Clermont-Ferrand, France. This track presents very smooth curves, and the test was made at constant  
176 speed (100 kph). Three filters (FESTO, MS9-LFM-B, pore size:  $1 \mu\text{m}$ ) located between the nozzles and the  
177 vacuums allowed us to collect all the particles resulting from the contact between the tire and the road,  
178 including TRWP of the target tire as well as other nontire particles and possibly TRWP that were  
179 previously emitted by other vehicles and resuspended by our testing vehicle. These particles were stored  
180 for approximately 1 year in the dark at room temperature before the following separation steps.

181 The collected particles were then sieved with a  $250 \mu\text{m}$  sieve. The preserved part consisted of particles  
182 under  $250 \mu\text{m}$  and accounted for at least 90 wt% of the initial amount. TRWP were separated from the  
183 crude environmental sample by densitometry using a 500 mL separating glass funnel (Glassco). First, a  
184 NaCl aqueous solution with a density of  $1.18 \text{ g cm}^{-3}$  was used to separate TRWP from the lighter biomass.  
185 The sample mass was  $5.0000 \pm 0.0005 \text{ g}$  for a total volume of 200 mL. Because the particles are  
186 hydrophobic, 100 mL of the solution was added after the particles were in a beaker. The sample was  
187 stirred vigorously for 2 minutes and was placed in an ultrasonic bath for 1 minute. Then, the sample was  
188 transferred to the separating funnel and agitated for 3 minutes. The last 100 mL of the solution was  
189 added, and the separating funnel containing the sample was again agitated for 3 minutes. It was then  
190 left to rest overnight (approximately 15 hours). After density separation, the higher density fraction was  
191 recovered, filtered and rinsed using 250 mL of distilled water through a  $10 \mu\text{m}$  nylon filter (70 mm,  
192 Merck Millipore). Then, a NaI aqueous solution with a density of  $1.80 \text{ g cm}^{-3}$  was used to separate the  
193 TRWP from heavier mineral particles. The same operating conditions were used except that the  
194 recovered fraction was the lower density fraction. It was then filtered and rinsed following the same  
195 method as previously described. Approximately 2.6 g of the sample consisted of particles between  $1.18$   
196 and  $1.80 \text{ g cm}^{-3}$  and between 10 and  $250 \mu\text{m}$ .

197 After densitometry and before aging, extraction and analysis steps, particles were stored in the dark at  
198 room temperature for several months.

### 199 **2.1.3) Chemicals**

200 Analytical grade ethanol (GPR Rectapur, 99.8%) was purchased from VWR chemicals. Cyclohexane (ACS  
201 reagent grade, 99.8%) was purchased from Carlo Erba reagents. Ultra-pure water was obtained with a  
202 Millipore Synergy device.

203 1,3-Diphenylguanidine (DPG, 99.5%, CAS number 102-06-7) and 1,3-benzothiazole (BT, 96%, CAS 95-16-  
204 9) were purchased from Sigma Aldrich. Poly(1,2-dihydro-2,2,4-trimethylquinoline) (TMQ, 99%, CAS  
205 26780-96-1) and N-(1,3-dimethylbutyl)-N'-phenyl-p-phenylenediamine (6PPD, 98.5% CAS 793-24-8) were

206 acquired from Lanxess. N-Phenyl-N'-1,3-dimethylbutyl-p-quinonediimine (6QDI, CAS 52870-46-9) was  
207 provided by Michelin with >99% purity and synthesized according to patent WO9921826 A1. N-(1,3-  
208 Dimethylbutyl)-N'-phenyl-p-phenylenediamine-quinone (6PPD-quinone) was purchased from HPC with  
209 97% purity. Molecules will be further described in 2.4.2.

## 210 **2.2) Aging**

211 Three types of aging were investigated with both CMTTP and TRWP. Before aging, the particles were  
212 stored at room temperature and protected from light. All aging experiments were performed under  
213 ambient atmosphere to be representative of outdoor conditions, where tire particles are found.

### 214 **2.2.1) Accelerated photochemical aging at 60 °C**

215 Particles were aged in an Atlas SEPAP 12-24 photoaging chamber at 60 °C. SEPAP 12-24 is a closed  
216 chamber with 4 mercury-vapor lamps. The spectrum of lamps can be seen in Figure SI 4. Generally,  
217 polymer films are placed vertically into the SEPAP 12-24. For particle photodegradation, a sample holder  
218 with a mirror (45° angle) was used to allow the study of a sample placed horizontally. A picture is shown  
219 in figure SI 5. A quartz cover slide with a 185 nm wavelength cutoff was placed on the sample holder to  
220 prevent the sample from flying off in the chamber. Three sample holders were placed simultaneously in  
221 the SEPAP chamber for each exposure time for repeatability. A total of 0.0500 g of particles was placed  
222 in each sample holder and deposited evenly on the surface (11 cm<sup>2</sup>). Samples were aged for 2, 4, 6, 8, 15,  
223 24, 48, 72, 120, 168 and 240 hours.

### 224 **2.2.2) Thermal aging at 60 °C**

225 Thermal aging was conducted in a Binder Standard-Incubator E53 with natural convection at 60±2 °C at  
226 the same temperature as for photoaging. This temperature was chosen because it is expected to be  
227 reached on the surface of the road during summer, implying that tire particles would be subject to  
228 thermal degradation<sup>48</sup>. Particles were dry-aged in glass crystallizers covered with aluminum foil, and an  
229 aliquot of 0.0500 ± 0.0001 g was collected after 12, 25, 52, 80 and 101 days. This sampling was made in  
230 triplicate at the same time.

### 231 **2.2.3) Natural outdoor aging**

232 The abovementioned artificially accelerated aging conditions were compared to natural weathering  
233 conditions in Clermont-Ferrand, France, by exposing both CMTTP and TRWP to natural elements from  
234 July 2021 to November 2021 in open glass jars with a diameter of 92.5 mm and a height of 95 mm.  
235 Under this condition, most of the powder is directly exposed to natural sunlight. The jars were placed at  
236 localization 45°45'50"N, 3°06'50"E. The solar radiation and the temperature were collected from the  
237 Observatoire de Physique du Globe de Clermont-Ferrand data and are presented in Figures SI 6 and SI 7.

238 Cryomilled tire tread particle samples were initially prepared with 0.2000±0.0002 g of particles in 60 mL  
239 of water. CMTTP is hydrophobic and has a density of approximately 1.2 g.cm<sup>-3</sup>, and the powder tends to  
240 accumulate at the bottom of the jar during most of the experiment. The samples were stored without a  
241 lid; therefore, they were subjected to UV light and weather, e.g., rain and water evaporation. Twelve jars  
242 were exposed to natural elements on the 2<sup>nd</sup> of July 2021 and were successively removed in triplicate  
243 after 21, 49, 98, and 133 days.

244 A second experiment was carried out with TRWP. Samples were initially prepared with  $0.1000 \pm 0.0002$  g  
245 of particles in 30 mL of water in the same previously described glass jars. Six jars were exposed to natural  
246 elements on 23 July 2021, and jars were removed in triplicate after 56 days and after 112 days.

247 After each removal, if any water was present in the jar, it was collected, filtered, and stored at  $-20$  °C.  
248 Particles were collected and dried in open air at ambient temperature, stored at room temperature and  
249 protected from UV light until extraction, which was carried out after a maximum of 2 weeks.

250

## 251 **2.3) Extraction from tire particles**

252 After being aged in dry conditions, particles (TRWP or CMTTP) were immersed for 24 hours at room  
253 temperature ( $20 - 25$  °C) in a solvent of choice (see 2.3.1 and 2.3.2). The 24-hour duration was chosen  
254 because the analyzed molecules did not show degradation over this period in the solvent, and the  
255 extraction from particles appeared to be maximal after 24 hours (figure SI 8). A ratio of  $0.1000$  g of  
256 particles to 15 mL of solvent was used. The samples were agitated at 550 rpm and protected from UV  
257 light during the 24 hours of extraction.

258 After the 24-hour extraction, the solvent was collected and filtered through a  $0.45$   $\mu\text{m}$  pore size syringe  
259 filter (Chromafil Xtra hydrophilic PTFE, 25 mm) and then stored in glass vials at  $-20$  °C until analysis. A  
260 maximum of 2 weeks was considered between aging and extraction. Extractions were made  
261 progressively as samples were taken out of aging. The extracts were stored for a maximum of 4 weeks  
262 before they were analyzed at  $-20$  °C. Furthermore, the stability of 6PPD under storage conditions at  $-$   
263  $20$  °C in cyclohexane/ethanol was verified (see SI paragraph 4.6 and Figure SI 12).

### 264 **2.3.1) In water**

265 Extractions were made in ultrapure water. As the aqueous leachates concentrations were low and close  
266 to the UHPLC-HRMS detection limit, extracts were preconcentrated 10 times prior to further analysis.  
267 One milliliter of aqueous leachate was evaporated with a Labconco Centrivap 10436E at  $35$  °C, and the  
268 resulting pellet was redissolved in  $100$   $\mu\text{L}$  of cyclohexane/ethanol prior to further UHPLC-HRMS analysis.

### 269 **2.3.2) In cyclohexane/ethanol**

270 Extractions were made with a mixture of apolar/polar solvent cyclohexane/ethanol with a 50:50v ratio.  
271 Each extract was analyzed by UHPLC-HRMS twice, one directly and one diluted 10 times in the same  
272 solvent, because the expected concentration for some molecules was above the linearity limits of  
273 concentration.

274

## 275 **2.4) Analytical analysis**

### 276 **2.4.1) DLS (particle size)**

277 The CMTTP size distribution (figure SI 1) was measured using a Malvern Mastersizer 3000 particle size  
278 analyzer. The analytical method was set up *via* laser light scattering with a liquid dispersion of the sample  
279 in ethanol, and the wavelengths of the sources were a  $632.8$  nm red laser and  $470$  nm blue LED.

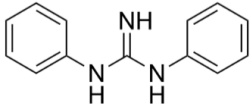
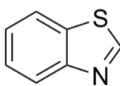
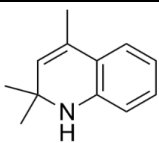
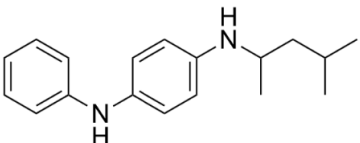
### 280 **2.4.2) UHPLC-HRMS**

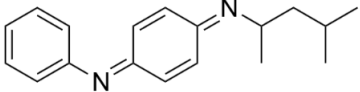
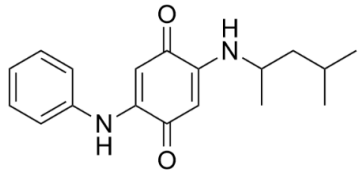


281 Samples and standards were injected with a volume of 5  $\mu\text{L}$  in ThermoScientific UHPLC Ultimate 3000  
 282 RSLC Ultra-High Performance Liquid Chromatography (UHPLC) equipment coupled with a  
 283 ThermoScientific Orbitrap Q-Exactive mass spectrometer (HRMS). The column used was a Phenomenex  
 284 Kinetex EVO C18 (100 x 2,1 mm; 1,7  $\mu\text{m}$ ). Mobile phases, gradients and flow rates are described in the  
 285 Supplementary Information. The electrospray ionization was in positive mode ESI +, and the detection  
 286 ranged from 90 to 400  $m/z$ . Details of the spectrometer conditions are described in SI paragraphs 4.1 and  
 287 4.2.

288 A majority of the analyses were grouped in batches for each kinetics. For each batch of analyzed  
 289 samples, calibration curves of the 6 standard molecules were prepared with concentrations of 5, 10, 50,  
 290 100, 500 and 1000  $\mu\text{g/L}$  in cyclohexane/ethanol. DPG, BT, TMQ, 6PPD and 6QDI were prepared within  
 291 the same calibration solutions, and 6PPD-quinone was prepared aside. The calibration curves were fitted  
 292 with a linear function and verified that  $R^2$  was  $> 0.997$ . As the TMQ standard is a mixture of monomer  
 293 and oligomers, calibration was carried out by correlating the monomer peak area to the total mass  
 294 concentration of the polymer sample (assuming a constant monomer mass fraction). The matrix effects  
 295 were considered non-significant via standard addition method for DPG, BT, TMQ, 6PPD and 6QDI, except  
 296 for 6PPD-quinone as it will be discussed later (see SI Paragraph 4.5, Figure SI 11 and Table SI 4).

297 Analyses were made using Thermo Xcalibur software. Calibration curves were verified with the Quan  
 298 Browser tool that was then used to quantify the concentration of each molecule in each extract using a  
 299 target method that was looking for the analyzed molecules via their retention time and measured mass  
 300 (shown in Table 1). This method was built by using molecular standards. Concentrations were calculated  
 301 by the mean of the triplicates, and the considered error is the standard deviation  $1\sigma$ .

Molecule (CAS)	Structural formula	Measured exact mass $[M+H]^+$	Retention time (min)	Neutral molecular formula
DPG (102-06-7)		212.1182	3.82	$\text{C}_{13}\text{H}_{13}\text{N}_3$
BT (95-16-9)		136.0216	5.45	$\text{C}_7\text{H}_5\text{NS}$
TMQ (monomer) (26780-96-1)		174.1277	8.63	$\text{C}_{12}\text{H}_{15}\text{N}$
6PPD (793-24-8)		269.2012	7.27	$\text{C}_{18}\text{H}_{24}\text{N}_2$

6QDI (52870-46-9)		267.1857	6.75	C <sub>18</sub> H <sub>22</sub> N <sub>2</sub>
6PPD-quinone		299.1753	8.69	C <sub>18</sub> H <sub>22</sub> N <sub>2</sub> O <sub>2</sub>

302

303 Table 1 Structural formula of 6 chemicals extracted from tires

304 Other molecules described by Seiwert *et al.*<sup>26</sup> and Müller *et al.*<sup>25</sup> were also investigated. A suspect  
305 screening of 6PPD and DPG degradation products was made based on the measured mass of ions  
306 reported by the previously mentioned authors. The hits were attributed to a retention time (RT), and the  
307 combination *m/z*-RT was used to look for these components in all the samples<sup>17,25,29,30</sup>. These molecular  
308 formulas, RT and *m/z*, are summarized in Tables SI 2 and SI 3.

309 Some components that showed peculiar kinetics during aging were specifically targeted for MS-MS  
310 fragmentation to have a better confidence level for these components. The selected *m/z* values of  
311 ionized components were 294, 310, 185, 205, 213, 281 and 186. The detailed parameters for the MS and  
312 MS-MS analyses were as follows: sheath gas flow rate (N<sub>2</sub>), 50 arbitrary units (AU); auxiliary gas flow rate  
313 (N<sub>2</sub>), 10 AU; capillary temperature, 320 °C; and spray voltage, 3.2 pos kV. For MS-MS, the resolution was  
314 set to 17500 at 200 *m/z*, and the collision energy was 35 AU. More information can be found in SI  
315 paragraph 4.3. The highest intensity fragment ions are summarized in Table SI 2.

316 The confidence levels of the different transformation products were attributed accordingly to  
317 Schymanski *et al.*<sup>49</sup> and are summarized in Tables SI 2 and SI 3.

318

## 319 2.5) Data fitting models

320 Decay exponential models were used to fit the degradation kinetics of the studied molecules.  
321 Parameters were calculated using the minpack package for R and the function nlsLM, which fits data  
322 with a Levenberg–Marquardt least square type algorithm.

323

## 324 3) Results and discussion

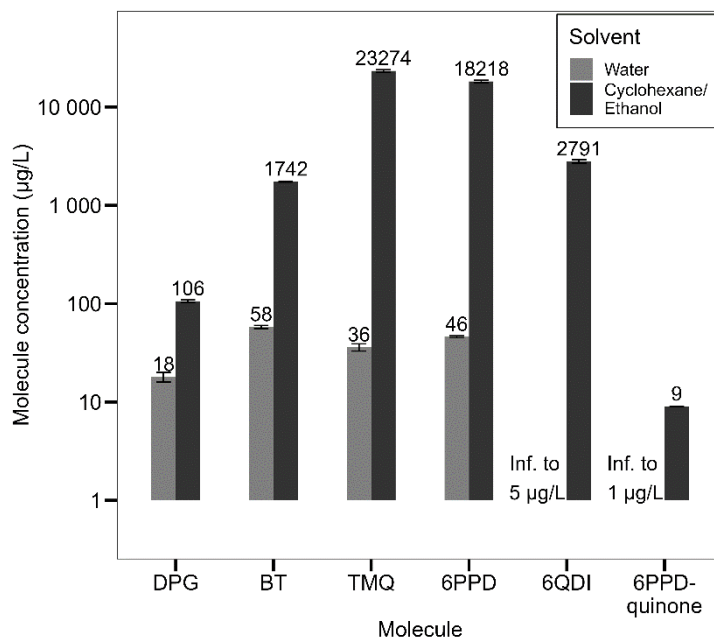
### 325 3.1) Leaching of molecules in cyclohexane/ethanol or in water and influence of extraction time

326 Additives from tire particles were extracted from CMTTP in water and in cyclohexane/ethanol. Among  
327 the molecules present in the UHPLC-HRMS analytical footprint of the water or cyclohexane/ethanol  
328 extracts, six molecules were targeted first and identified in particular, the vulcanization agents DPG and  
329 BT, the antiozonants/antioxidants TMQ and 6PPD, and the 6PPD-derived 6QDI and 6PPD-quinone<sup>30,31,35</sup>.  
330 First, extraction kinetics were carried out for up to 24 hours (Figure SI 8). To verify whether higher

331 extraction yields could be reached or if some molecules could be unstable<sup>36,37,39</sup> under prolonged  
332 extraction time at ambient temperature, a complementary 7-day extraction was carried out (results not  
333 shown). After 7 days of extraction, the concentration of DPG was still slightly increasing, and the  
334 concentrations of BT, TMQ and 6PPD were stable, but for 6QDI and 6PPD-quinone, an increase in  
335 concentration was also observed between 24 h and 7 days. The increase in 6QDI and 6PPD-quinone  
336 concentrations could be linked to either further extraction of these molecules or degradation of the  
337 parent 6PPD molecule during the extraction. For all the subsequent aging experiments, it was therefore  
338 chosen to systematically extract chemicals from CMTTP and TRWP for 24 h in cyclohexane/ethanol.

339 Water extraction experiments aimed at providing an order of magnitude of the leachability of molecules  
340 typically found in the tire particles in a closed-loop aqueous environment. Extractions in water were also  
341 carried out for 24 h. As expected, the concentrations of the 6 chemicals in water extracts were lower  
342 than those observed in cyclohexane/ethanol (Figure 1), with recovered concentrations below 100 µg/L  
343 for the 6 molecules. For instance, the TMQ concentration was approximately 1000 times lower in the  
344 water extracts than in cyclohexane/ethanol, while 6QDI and 6PPD-quinone were below the limit of  
345 detection. This can result from a lower extraction capacity in water, a poorer solubility and/or stability of  
346 the molecules in water. Among the 6 molecules investigated, DPG presents the highest concentration  
347 ratio between water and cyclohexane/ethanol, which is consistent with its higher polarity, based on log  
348 Kow or logD as calculated by Müller *et al.*<sup>25</sup> and its higher water solubility and stability (Table SI 1).  
349 Hence, provided water stability, the concentration ratio between water and cyclohexane/ethanol could  
350 provide insight into how the molecules share between the rubber and the water phase in environmental  
351 conditions and thus how potentially mobile they are toward the aqueous phase.

352 Overall, the total amount recovered for these 6 molecules in the cyclohexane/ethanol extracts of the  
353 native CMTTP represents approximately 46000 µg/L, i.e., *ca.* 0.7 wt% of the particles (Figure 1). In  
354 comparison, approximately 1 to 3 wt% of tire tread consists of protective molecules (e.g., TMQ, 6PPD),  
355 and 1 to 5 wt% is attributed to vulcanization components (e.g., DPG, CBS, BT)<sup>22,23,50</sup>. Therefore, based on  
356 the tread formulation, the 0.7 wt% recovered amount of these chemicals only represents a minor  
357 fraction (*ca.* 10 to 35 %) of the initial amount used for tire tread production. The degradation or reaction  
358 of these molecules during the manufacturing process (e.g., mixing, extrusion, curing) can explain the  
359 lower concentration of additives found in CMTTP<sup>51</sup>. This underlines the necessity to investigate  
360 degradation components in the analytical footprint of CMTTP. Further analysis of the measured mass of  
361 ions and the description of various chemical components by Müller *et al.*<sup>25</sup> or Seiwert *et al.*<sup>26</sup> make it  
362 possible to study other molecules in the following aging experiments with CMTTP.

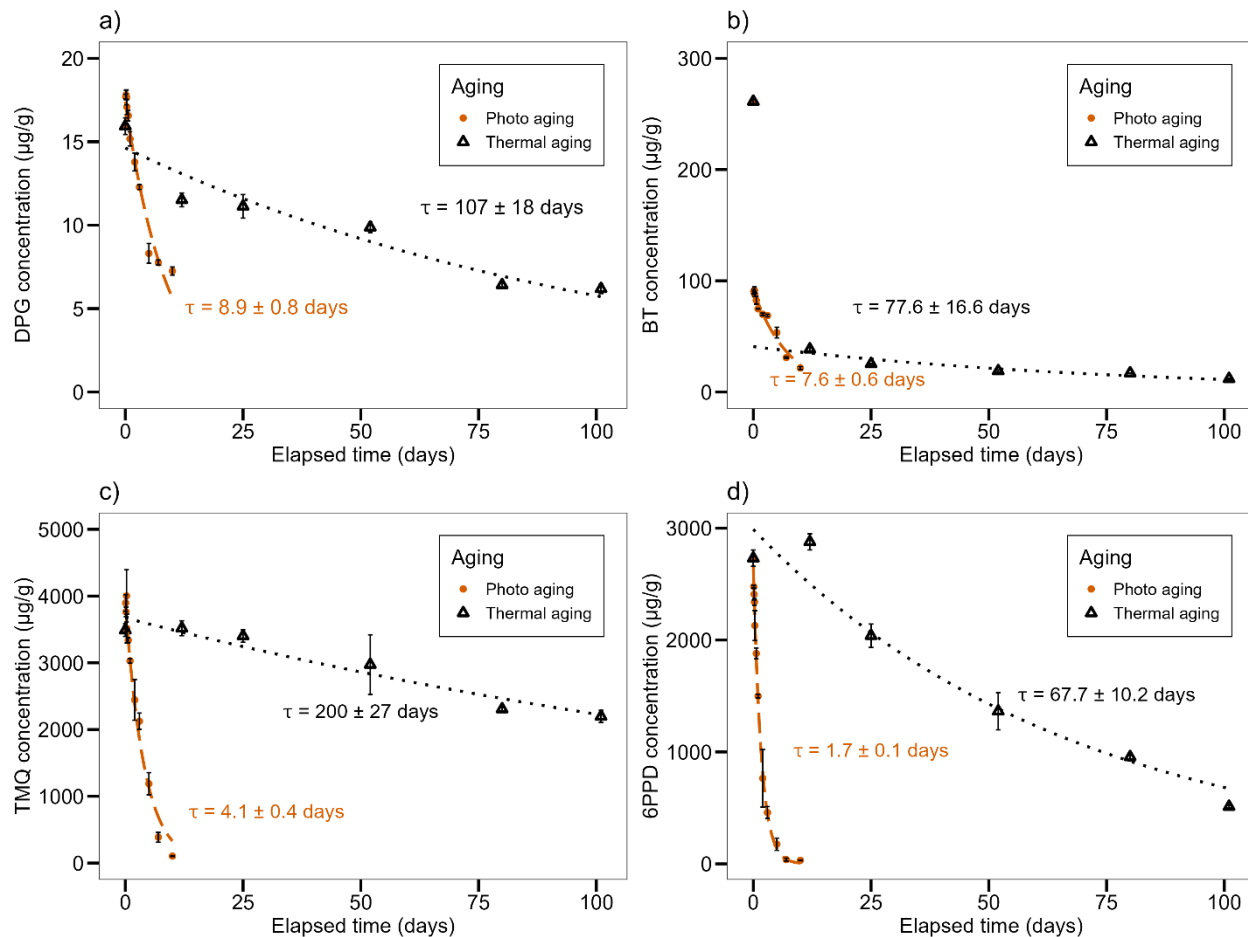


363  
 364 Figure 1: Concentrations of DPG, BT, TMQ, 6PPD, 6QDI, and 6PPD-quinone recovered from nonartificially aged CMTTP after a  
 365 24 h extraction in water or cyclohexane/ethanol. Extractions were made with 0.1 g of powder in 15 mL of solvent in the dark at  
 366 room temperature.

367 **3.2) Thermal and photochemical aging of CMTTP under accelerated conditions**

368 **3.2.1) Evolution of DPG, BT, TMQ and 6PPD concentrations upon aging**

369 The residual concentrations of DPG, BT, TMQ and 6PPD in CMTTP were measured at various stages of  
 370 thermal or photochemical aging by cyclohexane/ethanol extractions and LC-MS analysis. Before aging,  
 371 the CMTTP was kept at room temperature in the dark to limit degradation. The photoaging experiments  
 372 carried out with Atlas SEPAP 12-24 allowed faster degradation than in the environment. An acceleration  
 373 factor for polyolefins is estimated at approximately 12 between the SEPAP equipment and a continental  
 374 climate of central France<sup>52</sup>. For thermoaging, the chosen temperature (60 °C) is the same as for  
 375 photoaging. Kinetics of degradation were performed over 12 days and 101 days for photo- and  
 376 thermoaging, respectively, and the given concentrations correspond to the amount of each chemical  
 377 extracted by a mixture cyclohexane/ethanol for 24 h at room temperature under continuous stirring.  
 378 Concentrations of DPG, BT, TMQ and 6PPD decrease with time (Figure 2) with both photo- and  
 379 thermoaging (e.g., 6PPD reaches a nondetectable concentration under photo degradation after 7 days).  
 380 In this discussion, the terms “thermoaging” and “photo-aging” refer to the aging treatment to which the  
 381 particles were submitted, i.e., aging in an oven and in a SEPAP chamber. The terms “thermo  
 382 degradation” and “photo degradation” refer to the degradation that the particle and additives undergo  
 383 during aging. Photoaging is carried out at 60 °C and therefore can lead to a combination of both thermal  
 384 and photodegradation. Degradation can refer to multiple types of mechanisms, such as photooxidation  
 385 or thermooxidation<sup>38</sup>. In this discussion, degradation refers to the acknowledgment of a decrease in the  
 386 concentration of additives with time.



388

389 Figure 2: Evolution of the concentrations of a) DPG, b) BT, c) TMQ, and d) 6PPD extracted from CMTTP after various exposure  
 390 times to thermo or photoaging. Extractions were performed in cyclohexane/ethanol in the dark at room temperature for 24 h.  
 391 Concentrations are given in  $\mu\text{g}$  of the selected additive per g of CMTTP.

392 The concentration profiles were fitted with a single exponential decay [Equation 1].

$$393 \quad C(t) = C_0 * e^{-t/\tau} \text{ [Equation 1]}$$

394 where  $C(t)$  is the concentration of the molecule at a given time  $t$ ,  $C_0$  is the concentration at the beginning  
 395 of the degradation experiment and  $\tau$  is the time constant.  $\tau$  calculated for both photo- and thermoaging  
 396 are given in Figure 2 for each chemical.

397 Concentrations of DPG, BT, 6PPD and TMQ present different dissipation rates. In any case,  $\tau$  is lower than  
 398 10 days under accelerated photooxidative conditions, while a slower process was observed under purely  
 399 thermooxidative aging conditions, with calculated  $\tau$  spanning from 67.7 and 200 days for 6PPD and TMQ,  
 400 respectively.

401 A peculiar profile was noticed for BT under both types of aging, where a first drop in concentration was  
 402 observed immediately after the first sampling point, with an initial fast decrease of approximately 40%  
 403 followed by a slower dissipation profile. The experiment was conducted at 60 °C in both cases, and BT  
 404 was volatile<sup>29</sup> (vapor pressure 0.95 hPa at 50 °C)<sup>53</sup>. This initial concentration decrease in BT could result  
 405 from partial volatilization of the molecule. The rest of the kinetics being slower is probably induced by a

406 different dissipation mechanism. The choice was made for BT to take the first point out of the modeled  
407 kinetics. The  $\tau$  of BT might thus be overestimated since it does not consider the initial drop in  
408 concentration.

409 As thermoaging and SEPAP aging were operated at the same temperature, it was considered that the  
410 comparison between both aging experiments provides insight into the specific contribution of  
411 accelerated photooxidation.

412 The purpose of 6PPD and TMQ is to inactivate radicals or to form stable radicals<sup>35,39</sup> and to protect the  
413 elastomer phase from radical chain oxidation and ozonolysis. They react preferably with radicals formed  
414 by UV radiation. Therefore, a high rate of degradation was expected for TMQ and 6PPD, which was  
415 verified under photoaging because they have  $\tau_{\text{photo}}$  values of 4.1 and 1.7 days, respectively. Moreover,  
416 these molecules degrade slower under thermal aging, as it was observed that  $\tau_{\text{thermo}}/\tau_{\text{photo}}$  of TMQ and  
417 6PPD are approximately 50 and 40, respectively.

418 DPG is mainly used as a vulcanization agent. BT, on its side, is a decomposition product of CBS that is  
419 present in the tire tread immediately after the manufacturing processes<sup>24</sup> and is considered an initial  
420 product in this study. It was observed that DPG and BT have  $\tau_{\text{photo}}$  values of 8.9 and 7.6 days, respectively,  
421 while  $\tau_{\text{thermo}}/\tau_{\text{photo}}$  values are 12 and 10. Therefore, the degradation of these molecules is also  
422 considerably faster under accelerated photoaging than thermoaging.

423 Because the experiments were made at the same temperature and the ratio  $\tau_{\text{thermo}}/\tau_{\text{photo}}$  is between 10  
424 and 50 for BT, DPG, TMQ and 6PPD, one could hypothesize that photochemical aging leads to a drastic  
425 loss of antioxidants and residual additives. The four additives are chromophore species reacting with  
426 oxidizing species to give oxidation products, and these reactions may be enhanced by the UV radiation  
427 provided in the SEPAP chamber. This leads to the formation of radicals that are unstable and highly  
428 reactive, leading to the formation of transformation products. The degradation products of 6PPD after  
429 ozonation experiments are the most regularly described in the literature<sup>26,54</sup>. The case of DPG was  
430 recently described<sup>25</sup>. BT<sup>55</sup> and TMQ<sup>56</sup> degradation, on the other hand, are not well studied.  
431 Consequently, the presence of numerous degradation products for various initial additives is often still  
432 unrecognized. The next section will thus discuss the detection of DPG- and 6PPD-derived products.

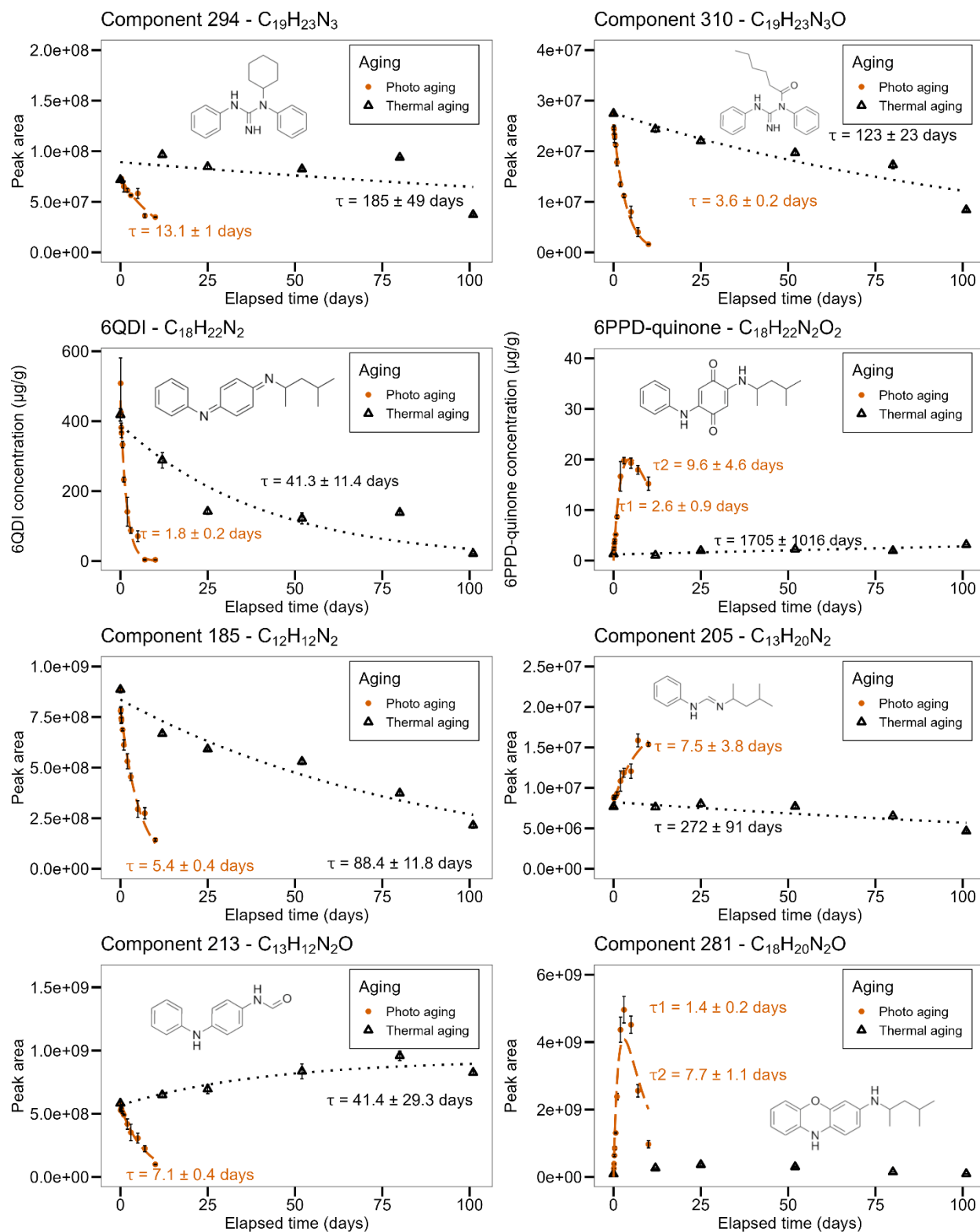
### 433 3.2.2) Transformation products of DPG and 6PPD

434 A suspect screening of transformation products was performed where molar mass ( $m/z$ ) of ionized  
435 components were targeted and associated with a retention time. Components were then named after  
436 the  $m/z$  of their ionized detected form, as retrieved in the chromatograms, e.g., Component 213 stands  
437 for  $m/z$  213.1019, RT = 6.78 min,  $C_{13}H_{13}N_2O$ . Details ( $m/z$ , RT, molecular formula, highest intensity  
438 fragment ions and confidence level) for all transformation products studied in this work can be found in  
439 Tables SI 2 and SI 3.

440 While the effects of the sample matrix on the ionization in the ESI source were non-significant for the 4  
441 previously studied molecules (DPG, BT, TMQ and 6PPD), this could not be verified for all the  
442 transformation products. The absence of matrix effect on 6QDI was verified (see figure SI 11). However,  
443 the standard addition plot for 6PPD-quinone was slightly nonlinear (see figure SI 11). Therefore, the  
444 absolute concentrations discussed below should be considered with caution from a quantitative  
445 standpoint for 6PPD-quinone and for other transformation products for which no standard molecule was  
446 used.

447 The transformation products studied here could be both produced and consumed during photo- and  
448 thermoaging. Various concentration profiles were observed depending on the chemicals (Figure 3).  
449 Several kinetic models have been proposed for intermediate products upon aging. The initial  
450 concentration corresponds to the amount of the chemical in the CMTTP after being stored in the dark at  
451 room temperature. When starting the additional aging, the reaction rates of the production(s) and  
452 consumption(s) of the different chemicals are modified, inducing a change in their concentrations. As  
453 observed for DPG and 6PPD, the concentration can decrease exponentially with time for both photo- and  
454 thermoaging, but some chemicals also present an initial increase in concentration in the photoaging  
455 experiment (e.g., 6PPD-quinone) or a continuous increase over the 101 days of the experiment in  
456 thermoaging (e.g., Component 213).

457 Out of the 38 6PPD-transformation products identified by Seiwert *et al.*<sup>26</sup>, 17 matched with components  
458 present in our samples, including 6QDI and 6PPD-quinone. Eleven of them are presented in Figure SI 13,  
459 and 6 of them are presented in Figure 3 because of their distinctive degradation profiles. The  
460 nondetection of the other 21 6PPD-derived products reported by Seiwert *et al.* could be assigned to  
461 either sensitivity matter (i.e., concentrations below the limit of detection) or to distinct experimental  
462 setup (ozonation of pure 6PPD solutions or films<sup>26</sup> vs. aging of complex particles in this study). Similarly, a  
463 suspect screening list of DPG-transformation products was used based on those identified by Müller *et al.*<sup>25</sup>,  
464 leading to 2 hits with Components 294 and 310, as presented in Figure 3.



465

466 Figure 3: Evolution of the concentrations of different degradation products as a function of CMTTP exposure time to thermo or  
 467 photoaging and measured after a 24 h extraction in cyclohexane/ethanol. Components 294 and 310 correspond to targeted  
 468 degradation products of DPG as described by Müller<sup>25</sup>. Standards were used to quantify the concentrations of 6QDI and 6PPD-



469 quinone only. Components 185, 205, 213 and 281 correspond to the targeted degradation products of 6PPD, as reported by  
470 Seiwert *et al.*<sup>26</sup> The molecular structure of Component 185 is not given due to a confidence level inferior to 3.

471  
472 Considering the different concentration profiles, other simple models were used to estimate the rate of  
473 degradation/production. Molecules showing an increase followed by a decrease in concentration were  
474 fitted by a sum of two exponentials, with [Equation 2]:

$$475 \quad C(t) = C_x (-\exp^{-t/\tau_1} + \exp^{-t/\tau_2}) \text{ [Equation 2]}$$

476 where  $\tau_1$  and  $\tau_2$  are the parameters describing the formation and dissipation rate of the molecule,  
477 respectively, and  $C_x$  is a constant related to the concentration of the molecule.

478 Molecules showing only an increase in concentration were fitted with a single exponential, with  
479 [Equation 3]:

$$480 \quad C(t) = (C_0 - C_f) * (\exp^{-t/\tau}) + C_f \text{ [Equation 3]}$$

481 where  $C_0$  is the calculated initial value of concentration and  $C_f$  is the calculated final value of  
482 concentration.

#### 483 **DPG-derived products**

484 Components 294 and 310 (Figure 3) were reported by Müller *et al.* as ions  $C_{19}H_{24}N_3^+$  and  $C_{19}H_{24}N_3O^+$ ,  
485 which would correspond to molecules  $C_{19}H_{23}N_3$  and  $C_{19}H_{23}N_3O$ , respectively. Müller *et al.*<sup>25</sup> described the  
486 former as one of the highest intensities leachable in their study. Both molecules are supposed to be DPG-  
487 derived products (putatively N-cyclohexyl-diphenylguanidine and N-carbonyl-diphenylguanidine resp.)  
488 and show a rapid decrease in their concentrations under photoaging ( $\tau$  of 13.1 and 3.6 days) and a  
489 slower decrease under thermoaging, similar to the concentration profile of DPG (Figure 2). Müller *et al.*  
490 assumed that these molecules would form during the tire tread manufacturing process by condensing  
491 with other vulcanization agents<sup>25</sup>. This is consistent with the nonzero concentrations observed in this  
492 study for these molecules prior to the beginning of accelerated aging. Therefore, accelerated photo and  
493 thermal aging may not be the main reason why these molecules are forming, but they degrade  
494 themselves at rates similar to those of DPG ( $\tau_{DPG} = 8.9$  and 107 days under accelerated photo and  
495 thermal aging).

#### 496 **6PPD-derived products**

497 The initial concentration of 6QDI was quite significant (420  $\mu\text{g/g}$ ) compared to the parent 6PPD  
498 concentration (2700  $\mu\text{g/g}$ ), and an equilibrium exists between these two molecules<sup>26,40</sup>. 6PPD and 6QDI  
499 present similar dissipation rates under photoaging (*ca.* 1.7 days) and under thermal aging (67 and 41  
500 days, respectively). The ratio 6QDI/6PPD remains approximately constant during accelerated aging  
501 experiments. A similar behavior was observed with Component 185<sup>32,36</sup>, although with slower dissipation  
502 rates by a factor of *ca.* 2 compared to 6PPD or 6QDI. The transformation from 6PPD to 6QDI involves a  
503 radical reaction followed by rearrangements, while the transformation from 6PPD to supposedly 4-ADPA  
504 (Component 185) involves the loss of the alkyl chain that leads to the formation of a primary amine.

505 On the other hand, the concentration of 6PPD-quinone initially increased upon both aging types with  
506 very different rates. The concentration increased from 1.3 to 20  $\mu\text{g/g}$  under accelerated photoaging after

507 5 days. In comparison, the concentration of 6PPD decreased from 2700 to 175  $\mu\text{g/g}$  after 5 days and to  
508 30  $\mu\text{g/g}$  after 10 days under accelerated photoaging. The formation rate of 6PPD-quinone is similar to  
509 the dissipation rate of 6PPD (2.6 days vs. 1.7 days). Based on the quinone formation pathway<sup>26</sup>, the 6PPD  
510 stock depletion induced by its degradation leads to a lower production rate of 6PPD-quinone, whose  
511 concentration reaches a maximum at 5 days. The concentration of 6PPD-quinone is always much smaller  
512 than the concentration of 6PPD; it is probably related to the numerous concurrent 6PPD degradation  
513 pathways leading to the production of molecules other than 6PPD-quinone but also to the degradation  
514 of 6PPD-quinone itself, which would be comparably fast compared to its production. With regard to the  
515 thermoaging experiment, 6PPD-quinone presented a slow and continuous concentration increase, with  
516 3  $\mu\text{g/g}$  reached after 101 days (compared to 20  $\mu\text{g/g}$  under photoaging after 5 days), which is still 170  
517 times lower than the 6PPD concentration within CMTTP at that time. In fact, the concentration of a few  
518 other transformation products, such as 6PPD-quinone, continuously increased during the 101 days of the  
519 thermal aging experiment, while it decreased under accelerated photo aged conditions. This is the case  
520 with Component 213, whose concentration is halved within 5 days under photoaging ( $\tau = 7.1$  days), while  
521 it increases at 60 °C in the absence of light. According to the hypothetical pathway reported by Seiwert  
522 *et al.*<sup>26</sup>, the formation of Component 213 would result from formaldehyde addition to 6PPD and then  
523 from the scission of the alkyl chain. The build-up of Component 213 observed under thermoaging shows  
524 that this pathway does occur at 60 °C, while the decrease in concentration observed at the same  
525 temperature under UV irradiation shows that its degradation becomes faster than its formation under  
526 these conditions. These molecules (6PPD-quinone, Component 213) are therefore mainly degraded in  
527 the presence of light and could persist in the environment while accumulating in a dark spot.

528 The reported Component 281<sup>26,34</sup> would consist of another transformation product derived from 6PPD  
529 ozonation via the same quinone pathway as the one leading to 6PPD-quinone. In the present study, its  
530 concentration profile was observed to be very similar to that of 6PPD-quinone, and both molecules  
531 reached their maximal concentration at 5 days under accelerated photoaged conditions.

532 As further evidence of the degradation of 6PPD-quinone, a suspect screening approach was also carried  
533 out by searching for the ozonation products of 6PPD quinone reported in the literature<sup>26</sup> and led to the  
534 detection of Component 205. Its increasing concentration profile under photoaging is similar to that of  
535 6PPD-quinone but with a lag, i.e., higher time constant  $\tau$  and no bell-shaped curve observed within the  
536 12-day duration of the experiment. These observations would be consistent with the assignment of  
537 Component 205 as a 6PPD-quinone putative transformation product.

538 The main conclusion of these accelerated aging studies is that additives of tire tread particles degrade  
539 under both photo- and thermoaging. In particular, DPG and 6PPD degradation leads to the appearance  
540 of several degradation products. While degradation of molecules such as DPG and 6PPD occurred within  
541 a few days in the accelerated photoaging experiment, their transformation products can have a longer  
542 persistence, such as Component 205, whose concentration is still rising after 12 days, while 6PPD  
543 decreased from 2700 to 30  $\mu\text{g/g}$ . These laboratory aging experiments were then completed with an  
544 outdoor aging study.

545

546

547

548

549 **3.3) Outdoor aging of CMTTP**

550 Degradation of CMTTP over a 4-month outdoor aging period was assessed by using the same analytical  
 551 protocol as the one used for accelerated aging (i.e., extraction in cyclohexane/ethanol and LC–MS). The  
 552 data are given in Figures SI 14, SI 15 and SI 16, and the time constants ( $\tau$ ) obtained from simple models  
 553 (Equations 1-2) are summarized in Table 2.

554 The concentration profiles obtained under outdoor weathering were similar to the artificial photoaging  
 555 profiles for all the components discussed in the previous section (i.e., DPG, BT, TMQ, 6PPD and the  
 556 abovementioned transformation products). In terms of kinetics, each outdoor profile was systematically  
 557 comprised between the faster artificial accelerated photoaging degradation profile and the slower  
 558 thermoaging profile of the corresponding molecule. However, for BT,  $\tau_{\text{outdoor}}$  was not between  $\tau_{\text{thermo}}$  and  
 559  $\tau_{\text{photo}}$ , which might be explained by the fact that the first point of the kinetics was removed from the  
 560 calculation of  $\tau$ ; therefore, its estimation is less precise than for other molecules. The concentrations of  
 561 TMQ and 6PPD decreased by > 98% in less than 50 days of weathering, while DPG and BT concentrations  
 562 were reduced by 70% and 90%, respectively. Outdoor aging is thus faster than artificial thermoaging at  
 563 60 °C for these molecules, indicating that photodegradation is an essential degradation path under  
 564 outdoor weathering for the additives studied in this work.

565 6PPD and 6QDI also presented similar degradation rates under outdoor aging with a time constant of 1  
 566 week. Formation then dissipation of both 6PPD-quinone and Component 281 was also observed under  
 567 outdoor weathering, with a maximal concentration within CMTTP reached within 20 days for both  
 568 molecules versus 5 days under artificial photoaging. Component 205 presented a bell-shaped profile  
 569 similar to that of 6PPD-quinone under natural aging, while a decrease in concentration was not observed  
 570 after 10 days under accelerated photoaging.

Molecule	$\tau_{\text{photo}}$ (days)	$\tau_{\text{thermo}}$ (days)	$\tau_{\text{outdoor}}$ (days)	Ratio $\tau_{\text{thermo}}/\tau_{\text{photo}}$	Ratio $\tau_{\text{outdoor}}/\tau_{\text{photo}}$
DPG decrease	8.9 ± 0.8	107 ± 18	18.7 ± 5.3	12	2
BT decrease	7.6 ± 0.6	78 ± 17	126 ± 37	10	17
TMQ decrease	4.1 ± 0.4	200 ± 27	10.9 ± 0.2	49	3
6PPD decrease	1.7 ± 0.1	67.7 ± 10.2	7.1 ± 0.4	40	4
6QDI decrease	1.8 ± 0.2	41.3 ± 11.4	7.1 ± 0.8	23	4
6PPD-quinone increase	2.6 ± 0.9	1700 ± 1000	9.6 ± 5.8	>200	4

6PPD-quinone decrease	9.6 ± 4.6	-	26.2 ± 9.4	-	3
Component 294 decrease	13.1 ± 1.0	185 ± 49	78 ± 18	14	6
Component 310 decrease	3.6 ± 0.2	123 ± 23	11.9 ± 1.6	34	3
Component 185 decrease	5.4 ± 0.4	89 ± 12	13.7 ± 1.8	16	3
Component 205 increase	7.5 ± 3.8	-	27 ± 93	-	∅
Component 205 decrease	-	272 ± 91	45 ± 137	-	-
Component 213 increase	-	41.4 ± 29.3	-	-	-
Component 213 decrease	7.1 ± 0.4	-	13.1 ± 2.9	-	2
Component 281 increase	1.4 ± 0.2	*	15 ± 54	-	∅
Component 281 decrease	7.7 ± 1.1	*	17 ± 58	-	∅

571

572 Table 2: Comparison of concentration evolutions in CMTTP ( $\tau$ ) between accelerated photoaging (SEPAP at approximately 60 °C),  
573 thermoaging (60 °C in the dark) and natural aging. (-) Not observed in this aging condition. (\*) Not fittable. (∅) irrelevant to  
574 calculate due to uncertainty on the evaluation of  $\tau$

575 To our knowledge, this study is the first to provide an order of magnitude of the dissipation rate of tire  
576 tread additives and their transformation products (Table 2) as well as kinetic profiles of their degradation  
577 under natural outdoor weathering conditions, which could be representative of the ones encountered by  
578 TRWP on road or roadside soil surfaces. Concentrations of the studied additives (DPG, TMQ and 6PPD)  
579 are decreased by more than 50% within 20 days, and the concentrations of 17 out of 19 of their studied  
580 transformation products are also decreased by more than 50% within 50 days under natural aging  
581 conditions.

582 These results are consistent with Thomas *et al.*<sup>33</sup> who found that 6PPD and 6PPD-quinone could not be  
583 detected after artificial aging equivalent to 1 year in a natural environment. Concentration profiles  
584 observed by Unice *et al.*<sup>32</sup> are close to those observed under natural outdoor aging in this study for DPG  
585 and 6PPD. However, their experiments were carried out in an accelerated aging chamber for an  
586 equivalent of 3 years under natural conditions, and the kinetics observed in the present study are 10  
587 times faster than those for DPG and 3 times faster for 6PPD. This could be linked to experimental  
588 conditions, since this study was conducted in actual natural conditions, whereas their study was  
589 conducted in an artificial aging chamber.

590 Furthermore, Klöckner *et al.*<sup>34</sup> suggested potentially identifying markers for tire particles in the  
591 environment. Their selected markers included 6PPD-quinone and N-formyl-6PPD (Component 297 –  
592 figure SI 15), which were still persistent in their study after an accelerated photoaging of 72 hours at 32  
593 °C, corresponding to 7 weeks of sunshine duration in Germany. However, the present study showed that  
594 these two components are not stable under natural weathering, with Component 297 concentration  
595 undergoing, for instance, a 90% decrease in its initial concentration within 50 days, which raises the  
596 question of their relevance as persistent markers.

597

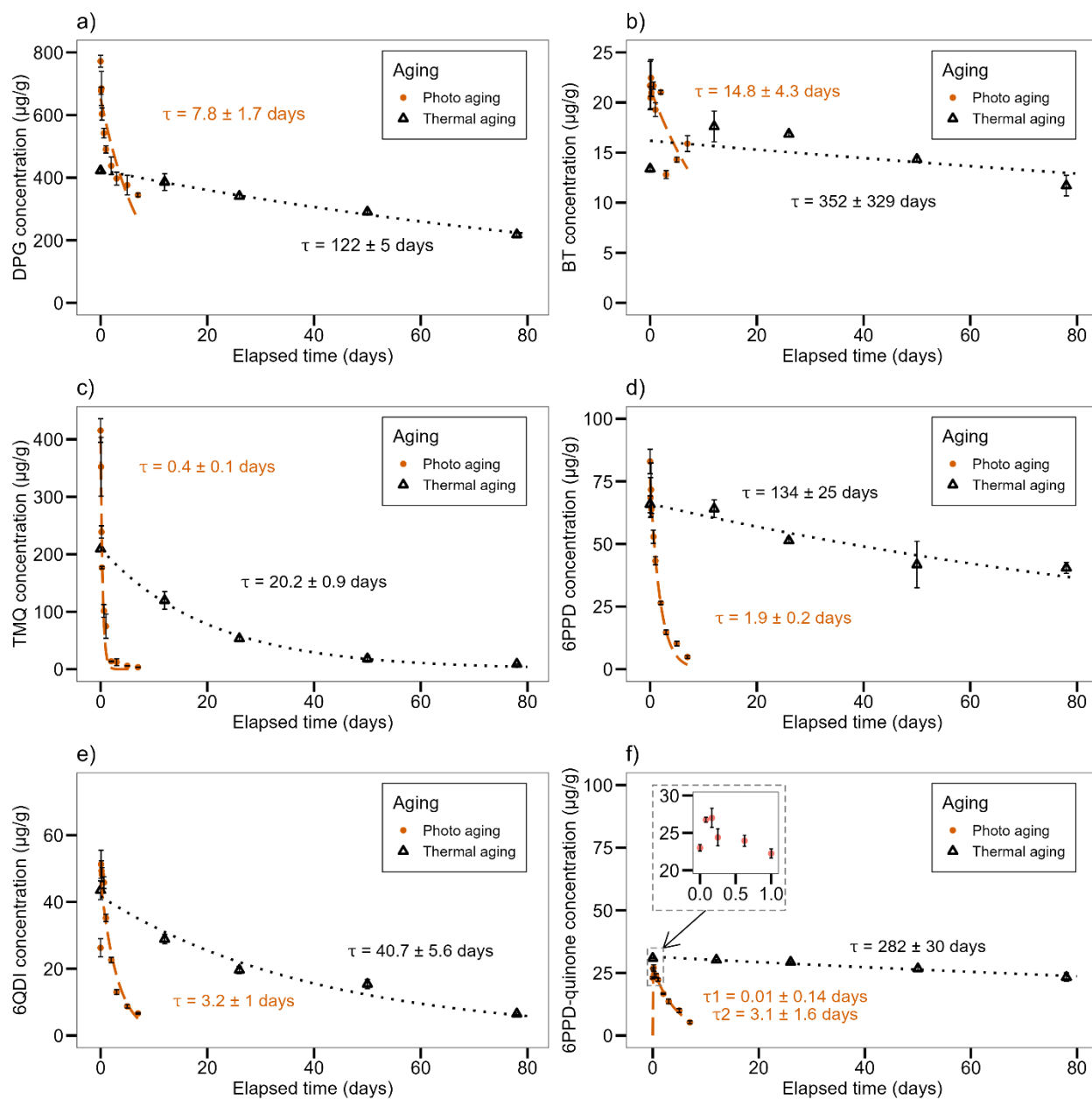
### 598 **3.4) Degradation of additives under accelerated and natural aging of TRWP**

599 TRWP were collected immediately after emission *via* an in-vehicle embedded system and were then  
600 stored in the dark at room temperature for 2.5 years. TRWP were then separated with densitometry.  
601 Following the abovementioned steps, the concentration within TRWP of a molecule relatively well  
602 soluble in water, such as DPG (Figure 1), could be underestimated because it was partially extracted in  
603 the aqueous solution used during the densitometry step. However, this should not change the kinetics  
604 results, since the studied phenomenon consists of additional aging to particles that were already partially  
605 aged. Moreover, the history of the TRWP *before* artificial aging is significantly different from that of the  
606 CMTTP. The latter were obtained from a new tire tread, whereas TRWP consist of a rubber material that  
607 experienced severe damage induced by friction on the rough road surface during tire rolling conditions<sup>2</sup>.  
608 Both the rubber compositions and ages of the starting materials used to produce CMTTP and TRWP were  
609 different, which might also contribute to explaining why the initial concentrations are different between  
610 CMTTP and TRWP for some molecules (e.g., DPG and BT).

611

#### 612 **3.4.1) Accelerated aging of TRWP**

613 The TRWP were subjected to identical artificial and natural aging to CMTTP. Both types of particles  
614 presented similar results with regard to the dissipation rate of the additives and transformation  
615 products. The evolution of the amount of chemicals extracted from TRWP after thermo and photoaging  
616 is presented in Figure 4 and Figure SI 17. The time constants ( $\tau$ ) are summarized in table SI 5.



617

618

619 Figure 4 Evolution of the concentrations of a) DPG, b) BT, c) TMQ, d) 6PPD, e) 6QDI and f) 6PPD-quinone as a function of TRWP  
 620 exposure time to photoaging and measured after a 24 h extraction in cyclohexane/ethanol in the dark.

621 For all the investigated molecules, the kinetics of degradation within TRWP showed similar behavior to  
 622 the one observed within CMTP, i.e., a faster degradation under accelerated photoaging with  $\tau_{\text{photo}}$   
 623 below 15 days. Degradation under thermoaging at 60 °C was slower, with  $\tau_{\text{thermo}}$  occurring between 20  
 624 days for TMQ and 282 days for 6PPD-quinone. The kinetics appeared to be similar to those observed  
 625 with CMTP for 6PPD, DPG and 6QDI; however, a large difference was observed with TMQ, whose  
 626 kinetics of degradation were 10 times faster in TRWP than in CMTP, both under accelerated thermo and  
 627 photoaging. For transformation products (Figures SI 17 and SI 18), the differences mostly lied in products  
 628 that had bell-shaped curves in CMTP, which presented a higher starting concentration in TRWP and

629 only a concentration decrease, meaning that the maxima were probably reached before the start of the  
630 experiments, during the previous lifespan of TRWP. However, the kinetics of appearance/disappearance  
631 are similar to those observed with CMTTP with the same order of magnitude of characteristic time  
632 constants ( $\tau$ ).

633 Interestingly, the ratio of 6PPD and 6PPD-quinone concentrations at the beginning of the aging  
634 experiments (*ca.* 2700 and 1  $\mu\text{g/g}$  resp.) is  $>1000$  in the case of CMTTP and is only approximately 3 with  
635 the TRWP used in this work (*ca.* 75 and 25  $\mu\text{g/g}$ , respectively). This is probably related to the different  
636 histories of both types of particles prior to our aging study and to the greater stability of 6PPD-quinone  
637 than 6PPD under the storage conditions (ambient atmosphere, room temperature and in the dark). This  
638 illustrates how degradation products are as important as the parent chemicals for the evaluation of the  
639 possible impact of TRWP on the environment.

#### 640 **3.4.2.) Outdoor aging of TRWP**

641 Outdoor aging of TRWP (Figures SI 19, SI 20, SI 21 and Table SI 5) showed that degradation rates were  
642 slower for most of the chemicals within TRWP than within CMTTP under natural weathering. However,  
643 for most of the studied molecules,  $\text{DT50}_{\text{outdoor}}$  was below 50 days, with the exception of BT, which had a  
644 slower rate of degradation. It was shown that the concentration of 6PPD-quinone decreased by 97% in 3  
645 months under natural weathering, which includes solar UV radiation. Under natural sunlight,  $\tau_{\text{outdoor}}$  of  
646 6PPD-quinone is 26 and 20 days with CMTTP and TRWP, respectively.

647 One significant difference between CMTTP and TRWP concerns the initial concentration of 6PPD-  
648 quinone. For CMTTP, despite a several-year-long storage period prior to this study, 6PPD-quinone was  
649 hardly detected at the beginning of our aging experiments, and its concentration increased from 1.3  $\mu\text{g/g}$   
650 to 20  $\mu\text{g/g}$  after 5 days of photoaging or to 15  $\mu\text{g/g}$  after 21 days of natural weathering. The DT50 was  
651 below 10-30 days under natural outdoor aging, while the concentration continuously increased under  
652 thermoaging (approximately 100-133 days were necessary to reach 5  $\mu\text{g/g}$ ). On the other hand, despite a  
653 shorter storage period prior to this study compared to CMTTP, the maximal concentration of 6PPD-  
654 quinone in TRWP was already reached prior to our additional aging experiments, as no bell-shaped  
655 concentration profile could clearly be observed, and the starting concentration was approximately  
656 30  $\mu\text{g/g}$ . The concentration of 6PPD-quinone decreased faster ( $\text{DT50} = 14 \pm 3$  days) under natural aging  
657 (Figure SI 19) in the presence of light than in the dark (DT50 estimated approximately 180 days at 60 °C).  
658 These results might indicate that 6PPD-quinone could have been produced before the collection of  
659 TRWP, i.e., during the tire use and could thus be already available in TRWP for leaching even before the  
660 particles are submitted to additional UV radiation. The concentration of 6PPD-quinone can then be  
661 reduced in the presence of light, whereas it can persist in the environment in the dark. Nevertheless, as  
662 the driving circuit used for TRWP collection was not cleared off prior to testing, it cannot be excluded  
663 that older TRWP originating from previous vehicles passing by were collected together with the target-  
664 tire TRWP. The former, having been exposed to on-road environmental aging for an undetermined  
665 period of time prior to collection, might be the actual source of the 6PPD-quinone initial concentration in  
666 our sample. Dosing 6PPD-quinone in the outermost layer of a tire treadband or TRWP collection from a  
667 road simulator laboratory free from any other polluting rubber sources would help to fill this knowledge  
668 gap.

669 This study also highlights that additives and transformation products should be used as markers only for  
670 fresh TRWP ( $< 3$  months old). Indeed, TRWP composition evolves under aging toward a cocktail of

671 transformation products that are not well known. Therefore, assessing the quantity of older TRWP can  
672 be complex. On the other hand, TRWP might not necessarily be exposed to UV radiation in their lifespan  
673 in the environment because they might be quickly wiped away by rainwater runoff and remain in  
674 sediments or soils where only temperature or microbial action could degrade them. In this study, it was  
675 shown that thermoaging is less efficient than photoaging to degrade the additives and degradation  
676 products of TRWP. Therefore, buried TRWP could lead to a slower degradation of additive molecules and  
677 transformation products - via abiotic pathways at least - and thus represent for a longer period of time a  
678 source of potentially leachable molecules, whose environmental impact might be of concern.

679 The comparison of the CMTTP vs. TRWP results produced in this study is limited by the fact that both  
680 types of particles originated from different starting material compositions. A proper comparison would  
681 be worth future prospects to confirm that despite their different physicochemical characteristics  
682 compared to TRWP<sup>2,46</sup>, the more readily accessible CMTTP may be used as a good model to investigate  
683 the aging of TRWP, at least for studying the fate of chemicals, identifying transformation products, and  
684 estimating trends and orders of magnitude.

685

#### 686 **4. Conclusion**

687 This study assessed the kinetics of abiotic degradation of various additives and transformation products  
688 within tire particles under three kinds of aging: accelerated photochemical and/or thermal aging and  
689 natural outdoor aging. Chemicals were extracted from aged particles with cyclohexane/ethanol solvent  
690 and analyzed using UHPLC-HRMS.

691 Concentration-time profiles of 23 chemicals were established for each type of aging experiment and  
692 particle (CMTTP and TRWP), among which 3 tire tread additives (DPG, 6PPD, TMQ) and 20  
693 transformation products (featuring 6PPD-quinone as well as 17 other 6PPD- or DPG-derivatives  
694 previously reported in the literature). DPG, 6PPD, TMQ and some transformation products decayed  
695 exponentially under the 3 types of aging. Their degradation rate was systematically higher under  
696 accelerated photoaging, with half-lives of a few days (1 to 9 days) versus dozens of days under pure  
697 thermal aging. The natural outdoor aging kinetics systematically lie between those 2 laboratory aging  
698 conditions.

699 Two chemicals reported as issued from the 6PPD ozonation putative quinone pathway, namely, 6PPD-  
700 quinone and Component 281, clearly presented bell-shaped concentration profiles within CMTTP when  
701 the particles were exposed to UV light. 6PPD-quinone concentration reached a maximal concentration  
702 within 5 days under artificial photoaging and after approximately 20 days under natural outdoor aging,  
703 whereas Component 205, supposedly formed from the parent 6PPD-quinone, presented similar but  
704 lagged concentration profiles. For TRWP, where the initial load of those 3 chemicals was higher than that  
705 in CMTTP, those bell-shaped profiles were hardly detected under artificial photoaging, and exponential  
706 decays were observed under outdoor aging (half-life ~2 days and 14 days, respectively). Under dark and  
707 purely thermal aging, the decay of 6PPD-quinone within TRWP was significantly slower (half-life ~195  
708 days), emphasizing a greater stability and persistence in environmental compartments without light and  
709 at lower temperatures.

710 From a qualitative standpoint, the more readily accessible CMTTP can be considered a reasonable proxy  
711 of TRWP to investigate the general fate of chemicals within rubber particles when the particles are



712 exposed to various aging conditions. Indeed, both involve similar chemical species and similar aging  
713 kinetics trends and orders of magnitude. Nevertheless, this study was limited from the quantitative  
714 standpoint by the use of CMTTP and TRWP originating from different starting material compositions and  
715 by matrix effects on ionization in the UHPLC-HRMS analysis, induced by the complex nature of the  
716 sample itself, that probably impaired the absolute quantitation of 6PPD-quinone. This work should thus  
717 be completed in the future to fill these gaps.

718 In terms of environmental significance, this study highlighted that TRWP composition varies dynamically  
719 over time and aging conditions, which could lead to potentially harmful effects (e.g., ecotoxicity induced  
720 by emergence of a specific transformation product) or beneficial effects (e.g., disappearance of  
721 components inhibiting biodegradation of other substrates or appearance of biodegradation promoters).  
722 In future prospects, similar studies could be coupled to biodegradation or ecotoxicity assays to shed light  
723 on the implication of the aging-induced variability of TRWP composition. This study also emphasized the  
724 particular impact of UV light on TRWP composition. This can provide guidance for potential mitigation  
725 strategies or help improve the modeling of particle environmental fate by accounting for the time spent  
726 under light exposure. Finally, the leachability of the investigated molecules in water was not fully  
727 addressed in this work and the assessment of the amount that could effectively leach in the environment  
728 along with aging would be worth future prospects.

729

### 730 **Declaration of competing interest**

731 The authors declare that they have no known competing financial interest that could have appeared to  
732 influence the reported work.

733

### 734 **Acknowledgment**

735 This study was funded by Michelin and ANRT. The authors gratefully acknowledge Manon Darnaud for  
736 technical support in MS-MS fragmentation results interpretation.

### 737 **Bibliography**

- 738 (1) Rogge, W. F.; Hildemann, L. M.; Mazurek, M. A.; Cass, G. R.; Simoneit, B. R. T. Sources of Fine  
739 Organic Aerosol. 3. Road Dust, Tire Debris, and Organometallic Brake Lining Dust: Roads as Sources  
740 and Sinks. *Environ. Sci. Technol.* **1993**, *27* (9), 1892–1904. <https://doi.org/10.1021/es00046a019>.
- 741 (2) Smith, R. W.; Veith, A. G. Electron Microscopical Examination of Worn Tire Treads and Tread  
742 Debris. *Rubber Chem. Technol.* **1982**, *55* (2), 469–482. <https://doi.org/10.5254/1.3535892>.
- 743 (3) Kreider, M. L.; Panko, J. M.; McAtee, B. L.; Sweet, L. I.; Finley, B. L. Physical and Chemical  
744 Characterization of Tire-Related Particles: Comparison of Particles Generated Using Different  
745 Methodologies. *Sci. Total Environ.* **2010**, *408* (3), 652–659.  
746 <https://doi.org/10.1016/j.scitotenv.2009.10.016>.
- 747 (4) Dannis, M. L. Rubber Dust from the Normal Wear of Tires. *Rubber Chem. Technol.* **1974**, *47* (4),  
748 1011–1037. <https://doi.org/10.5254/1.3540458>.
- 749 (5) Councell, T. B.; Duckenfield, K. U.; Landa, E. R.; Callender, E. Tire-Wear Particles as a Source of Zinc  
750 to the Environment. *Environ. Sci. Technol.* **2004**, *38* (15), 4206–4214.  
751 <https://doi.org/10.1021/es034631f>.

- 752 (6) Boulter, P. G. *A Review of Emission Factors and Models for Road Vehicle Non-Exhaust Particulate*  
753 *Matter*; PPR065; TRL Limited; p 88.
- 754 (7) Pohrt, R. TIRE WEAR PARTICLE HOT SPOTS – REVIEW OF INFLUENCING FACTORS. *Facta Univ. Ser.*  
755 *Mech. Eng.* **2019**, *17* (1), 17. <https://doi.org/10.22190/FUME190104013P>.
- 756 (8) Kole, P. J.; Löhr, A. J.; Van Belleghem, F.; Ragas, A. Wear and Tear of Tyres: A Stealthy Source of  
757 Microplastics in the Environment. *Int. J. Environ. Res. Public Health* **2017**, *14* (10), 1265.  
758 <https://doi.org/10.3390/ijerph14101265>.
- 759 (9) Vogelsang, C.; Lusher, A. L.; Dadkhah, M. E.; Sundvor, I.; Umar, M.; Ranneklev, S. B.; Eidsvoll, D.;  
760 Meland, S. *Microplastics in Road Dust – Characteristics, Pathways and Measures*; 7361–2019;  
761 Institute of Transport Economics Norwegian Centre for Transport Research, 2019.
- 762 (10) Bänisch-Baltruschat, B.; Kocher, B.; Stock, F.; Reifferscheid, G. Tyre and Road Wear Particles (TRWP)  
763 - A Review of Generation, Properties, Emissions, Human Health Risk, Ecotoxicity, and Fate in the  
764 Environment. *Sci. Total Environ.* **2020**, 137823. <https://doi.org/10.1016/j.scitotenv.2020.137823>.
- 765 (11) Wagner, S.; Hüffer, T.; Klöckner, P.; Wehrhahn, M.; Hofmann, T.; Reemtsma, T. Tire Wear Particles  
766 in the Aquatic Environment - A Review on Generation, Analysis, Occurrence, Fate and Effects.  
767 *Water Res.* **2018**, *139*, 83–100. <https://doi.org/10.1016/j.watres.2018.03.051>.
- 768 (12) Unice, K. M.; Weeber, M. P.; Abramson, M. M.; Reid, R. C. D.; van Gils, J. A. G.; Markus, A. A.;  
769 Vethaak, A. D.; Panko, J. M. Characterizing Export of Land-Based Microplastics to the Estuary - Part  
770 I: Application of Integrated Geospatial Microplastic Transport Models to Assess Tire and Road Wear  
771 Particles in the Seine Watershed. *Sci. Total Environ.* **2019**, *646*, 1639–1649.  
772 <https://doi.org/10.1016/j.scitotenv.2018.07.368>.
- 773 (13) Unice, K. M.; Weeber, M. P.; Abramson, M. M.; Reid, R. C. D.; van Gils, J. A. G.; Markus, A. A.;  
774 Vethaak, A. D.; Panko, J. M. Characterizing Export of Land-Based Microplastics to the Estuary - Part  
775 II: Sensitivity Analysis of an Integrated Geospatial Microplastic Transport Modeling Assessment of  
776 Tire and Road Wear Particles. *Sci. Total Environ.* **2019**, *646*, 1650–1659.  
777 <https://doi.org/10.1016/j.scitotenv.2018.08.301>.
- 778 (14) Cao, G.; Wang, W.; Zhang, J.; Wu, P.; Zhao, X.; Yang, Z.; Hu, D.; Cai, Z. New Evidence of Rubber-  
779 Derived Quinones in Water, Air, and Soil. *Environ. Sci. Technol.* **2022**, *56* (7), 4142–4150.  
780 <https://doi.org/10.1021/acs.est.1c07376>.
- 781 (15) Zhang, Y.; Xu, C.; Zhang, W.; Qi, Z.; Song, Y.; Zhu, L.; Dong, C.; Chen, J.; Cai, Z. Phenylenediamine  
782 Antioxidants in PM 2.5 : The Underestimated Urban Air Pollutants. *Environ. Sci. Technol.* **2021**,  
783 *acs.est.1c04500*. <https://doi.org/10.1021/acs.est.1c04500>.
- 784 (16) Panko, J. M.; Chu, J.; Kreider, M. L.; Unice, K. M. Measurement of Airborne Concentrations of Tire  
785 and Road Wear Particles in Urban and Rural Areas of France, Japan, and the United States. *Atmos.*  
786 *Environ.* **2013**, *72*, 192–199. <https://doi.org/10.1016/j.atmosenv.2013.01.040>.
- 787 (17) Wagner, S.; Klöckner, P.; Reemtsma, T. Aging of Tire and Road Wear Particles in Terrestrial and  
788 Freshwater Environments – A Review on Processes, Testing, Analysis and Impact. *Chemosphere*  
789 **2022**, *288*, 132467. <https://doi.org/10.1016/j.chemosphere.2021.132467>.
- 790 (18) Grasland, F.; Chazeau, L.; Chenal, J.-M.; schach, R. About Thermo-Oxidative Ageing at Moderate  
791 Temperature of Conventionally Vulcanized Natural Rubber. *Polym. Degrad. Stab.* **2019**, *161*, 74–84.  
792 <https://doi.org/10.1016/j.polymdegradstab.2018.12.029>.
- 793 (19) Baldwin, J. M.; Bauer, D. R. Rubber Oxidation and Tire Aging - A Review. **2008**.  
794 <https://doi.org/10.5254/1.3548213>.
- 795 (20) Jendrossek, D.; Birke, J. Rubber Oxygenases. *Appl. Microbiol. Biotechnol.* **2019**, *103* (1), 125–142.  
796 <https://doi.org/10.1007/s00253-018-9453-z>.
- 797 (21) Sommer, F.; Dietze, V.; Baum, A.; Sauer, J.; Gilge, S.; Maschowski, C.; Gieré, R. Tire Abrasion as a  
798 Major Source of Microplastics in the Environment. *Aerosol Air Qual. Res.* **2018**, *18* (8), 2014–2028.  
799 <https://doi.org/10.4209/aaqr.2018.03.0099>.

- 800 (22) Rodgers, B.; Waddell, W. The Science of Rubber Compounding. In *The Science and Technology of*  
801 *Rubber*; Elsevier, 2013; pp 417–471. <https://doi.org/10.1016/B978-0-12-394584-6.00009-1>.
- 802 (23) Wik, A.; Dave, G. Occurrence and Effects of Tire Wear Particles in the Environment – A Critical  
803 Review and an Initial Risk Assessment. *Environ. Pollut.* **2009**, *157* (1), 1–11.  
804 <https://doi.org/10.1016/j.envpol.2008.09.028>.
- 805 (24) *European Union Risk Assessment Report N-Cyclohexylbenzothiazol-2-Sulphenamide*; ECHA, 2005.
- 806 (25) Müller, K.; Hübner, D.; Huppertsberg, S.; Knepper, T. P.; Zahn, D. Probing the Chemical Complexity  
807 of Tires: Identification of Potential Tire-Borne Water Contaminants with High-Resolution Mass  
808 Spectrometry. *Sci. Total Environ.* **2022**, *802*, 149799.  
809 <https://doi.org/10.1016/j.scitotenv.2021.149799>.
- 810 (26) Seiwert, B.; Nihemaiti, M.; Troussier, M.; Weyrauch, S.; Reemtsma, T. Abiotic Oxidative  
811 Transformation of 6-PPD and 6-PPD Quinone from Tires and Occurrence of Their Products in Snow  
812 from Urban Roads and in Municipal Wastewater. *Water Res.* **2022**, *212*, 118122.  
813 <https://doi.org/10.1016/j.watres.2022.118122>.
- 814 (27) Evans, J. J. Rubber Tire Leachates in the Aquatic Environment. *Rev. Environ. Contam. Toxicol.* **1997**,  
815 *151*, 67–115. [https://doi.org/10.1007/978-1-4612-1958-3\\_3](https://doi.org/10.1007/978-1-4612-1958-3_3).
- 816 (28) Nelson, S. M.; Mueller, G.; Hemphill, D. C. Identification of Tire Leachate Toxicants and a Risk  
817 Assessment of Water Quality Effects Using Tire Reefs in Canals. *Bull. Environ. Contam. Toxicol.*  
818 **1994**, *52* (4). <https://doi.org/10.1007/BF00194146>.
- 819 (29) Reddy, C. M.; Quinn, J. G. Environmental Chemistry of Benzothiazoles Derived from Rubber.  
820 *Environ. Sci. Technol.* **1997**, *31* (10), 2847–2853. <https://doi.org/10.1021/es970078o>.
- 821 (30) Tian, Z.; Zhao, H.; Peter, K. T.; Gonzalez, M.; Wetzels, J.; Wu, C.; Hu, X.; Prat, J.; Mudrock, E.;  
822 Hettlinger, R.; Cortina, A. E.; Biswas, R. G.; Kock, F. V. C.; Soong, R.; Jenne, A.; Du, B.; Hou, F.; He, H.;  
823 Lundeen, R.; Gilbreath, A.; Sutton, R.; Scholz, N. L.; Davis, J. W.; Dodd, M. C.; Simpson, A.; McIntyre,  
824 J. K.; Kolodziej, E. P. A Ubiquitous Tire Rubber–Derived Chemical Induces Acute Mortality in Coho  
825 Salmon. *Science* **2021**, *371* (6525), 185–189. <https://doi.org/10.1126/science.abd6951>.
- 826 (31) Tian, Z.; Gonzalez, M.; Rideout, C. A.; Zhao, H. N.; Hu, X.; Wetzels, J.; Mudrock, E.; James, C. A.;  
827 McIntyre, J. K.; Kolodziej, E. P. 6PPD–Quinone: Revised Toxicity Assessment and Quantification with  
828 a Commercial Standard. *Environ. Sci. Technol. Lett.* **2022**, *9* (2), 140–146.  
829 <https://doi.org/10.1021/acs.estlett.1c00910>.
- 830 (32) Unice, K. M.; Bare, J. L.; Kreider, M. L.; Panko, J. M. Experimental Methodology for Assessing the  
831 Environmental Fate of Organic Chemicals in Polymer Matrices Using Column Leaching Studies and  
832 OECD 308 Water/Sediment Systems: Application to Tire and Road Wear Particles. *Sci. Total Environ.*  
833 **2015**, *533*, 476–487. <https://doi.org/10.1016/j.scitotenv.2015.06.053>.
- 834 (33) Thomas, J.; Moosavian, S. K.; Cutright, T.; Pugh, C.; Soucek, M. D. Investigation of Abiotic  
835 Degradation of Tire Cryogrinds. *Polym. Degrad. Stab.* **2022**, *195*, 109814.  
836 <https://doi.org/10.1016/j.polymdegradstab.2021.109814>.
- 837 (34) Klöckner, P.; Seiwert, B.; Wagner, S.; Reemtsma, T. Organic Markers of Tire and Road Wear  
838 Particles in Sediments and Soils: Transformation Products of Major Antiozonants as Promising  
839 Candidates. *Environ. Sci. Technol.* **2021**, *55* (17), 11723–11732.  
840 <https://doi.org/10.1021/acs.est.1c02723>.
- 841 (35) Datta, R. N.; Huntink, N. M.; Datta, S.; Talma, A. G. Rubber Vulcanizates Degradation and  
842 Stabilization. *Rubber Chem. Technol.* **2007**, *80* (3), 436–480. <https://doi.org/10.5254/1.3548174>.
- 843 (36) Lattimer, R. P.; Hooser, E. R.; Layer, R. W.; Rhee, C. K. Mechanisms of Ozonation of N-(1,3-  
844 Dimethylbutyl)-N'-Phenyl-p-Phenylenediamine. *Rubber Chem. Technol.* **1983**, *56* (2), 431–439.  
845 <https://doi.org/10.5254/1.3538136>.
- 846 (37) Layer, R. W.; Lattimer, R. P. Protection of Rubber against Ozone. *Rubber Chem. Technol.* **1990**, *63*  
847 (3), 426–450. <https://doi.org/10.5254/1.3538264>.

- 848 (38) Shelton, J. R. Aging and Oxidation of Elastomers. *Rubber Chem. Technol.* **1957**, *30* (5), 1251–1290.  
849 <https://doi.org/10.5254/1.3542760>.
- 850 (39) Shelton, J. R. Mechanism of Antioxidant Action in the Stabilization of Hydrocarbon Systems. *J. Appl.*  
851 *Polym. Sci.* **1959**, *2* (6), 345–350. <https://doi.org/10.1002/app.1959.070020616>.
- 852 (40) Ignatz-Hoover, F.; To, B. H.; Datta, R. N.; De Hoog, A. J.; Huntink, N. M.; Talma, A. G. Chemical  
853 Additives Migration in Rubber. *Rubber Chem. Technol.* **2003**, *76* (3), 747–768.  
854 <https://doi.org/10.5254/1.3547765>.
- 855 (41) Ignatz-Hoover, F.; Datta, R. Antidegradants Impact Thermal Oxidative Stability. *Rubber Plast. News*  
856 **2003**, 12.
- 857 (42) Ducháček, V.; Sošková, L.; Pospíšil, J.; Kuta, A.; Taimr, L.; Rotschová, J. Antioxidants and Stabilizers:  
858 Part CXII—Influence of 1-Phenylamino-4-(Sec-Alkylamino)-3,6-Bis(4-Phenylaminophenylimino)-1,4-  
859 Cyclohexadiene on the Vulcanization and Ageing of Natural Rubber. *Polym. Degrad. Stabifity* **1990**,  
860 *29* (2), 217–231. [https://doi.org/10.1016/0141-3910\(90\)90033-4](https://doi.org/10.1016/0141-3910(90)90033-4).
- 861 (43) Thorp, H. H. Erratum for the Report “A Ubiquitous Tire Rubber–Derived Chemical Induces Acute  
862 Mortality in Coho Salmon,” by Z. Tian, H. Zhao, K T. Peter, M. Gonzalez, J. Wetzell, C. Wu, X. Hu, J.  
863 Prat, E. Mudrock, R. Hettlinger, A. E. Cortina, R. G. Biswas, F. V. C. Kock, R. Soong, A. Jenne, B. Du, F.  
864 Hou, H. He, R. Lundeen, A. Gilbreath, R. Sutton, N. L. Scholz, J. W. Davis, M. C. Dodd, A. Simpson, J.  
865 K. McIntyre, E. P. Kolodziej. *Science* **2022**, *375* (6582), eabo5785.  
866 <https://doi.org/10.1126/science.abo5785>.
- 867 (44) Rauert, C.; Charlton, N.; Okoffo, E. D.; Stanton, R. S.; Agua, A. R.; Pirrung, M. C.; Thomas, K. V.  
868 Concentrations of Tire Additive Chemicals and Tire Road Wear Particles in an Australian Urban  
869 Tributary. *Environ. Sci. Technol.* **2022**. <https://doi.org/10.1021/acs.est.1c07451>.
- 870 (45) Hiki, K.; Yamamoto, H. Concentration and Leachability of N-(1,3-Dimethylbutyl)-N'-Phenyl-p-  
871 Phenylenediamine (6PPD) and Its Quinone Transformation Product (6PPD-Q) in Road Dust  
872 Collected in Tokyo, Japan. *Environ. Pollut.* **2022**, *302*, 119082.  
873 <https://doi.org/10.1016/j.envpol.2022.119082>.
- 874 (46) Cadle, S. H.; Williams, R. L. Environmental Degradation of Tire-Wear Particles. *Rubber Chem.*  
875 *Technol.* **1980**, *53* (4), 903–914. <https://doi.org/10.5254/1.3535066>.
- 876 (47) Biesse, F. Tire and Environment : Proposed Approach to Measure Real Life Particle Emissions from  
877 Tyres; Hanover, 2022.
- 878 (48) Higashiyama, H.; Sano, M.; Nakanishi, F.; Takahashi, O.; Tsukuma, S. Field Measurements of Road  
879 Surface Temperature of Several Asphalt Pavements with Temperature Rise Reducing Function.  
880 *Case Stud. Constr. Mater.* **2016**, *4*, 73–80. <https://doi.org/10.1016/j.cscm.2016.01.001>.
- 881 (49) Schymanski, E. L.; Jeon, J.; Gulde, R.; Fenner, K.; Ruff, M.; Singer, H. P.; Hollender, J. Identifying  
882 Small Molecules via High Resolution Mass Spectrometry: Communicating Confidence. *Environ. Sci.*  
883 *Technol.* **2014**, *48* (4), 2097–2098. <https://doi.org/10.1021/es5002105>.
- 884 (50) Wilder, C. R.; Haws, J. R. Performance of Tread Compounds in Various Tire Constructions. *Rubber*  
885 *Chem. Technol.* **1972**, *45* (1), 10–15. <https://doi.org/10.5254/1.3544691>.
- 886 (51) *Effects of Waste Tires, Waste Tire Facilities, and Waste Tire Projects on the Environment*; California  
887 Integrated Waste Management Board, 1996.
- 888 (52) Lemaire, J.; Arnaud, R.; Lacoste, J. The Prediction of the Long-Term Photoageing of Solid Polymers.  
889 *Acta Polym.* **1988**, *39* (12), 27–32. <https://doi.org/10.1002/actp.1988.010390106>.
- 890 (53) *European Chemicals Agency*. <http://echa.europa.eu/> (accessed 2022-05-02).
- 891 (54) Hu, X.; Zhao, H. N.; Tian, Z.; Peter, K. T.; Dodd, M. C.; Kolodziej, E. P. Transformation Product  
892 Formation upon Heterogeneous Ozonation of the Tire Rubber Antioxidant 6PPD (N-(1,3-  
893 Dimethylbutyl)-N'-Phenyl-p-Phenylenediamine). *Environ. Sci. Technol. Lett.* **2022**, *9* (5), 413–419.  
894 <https://doi.org/10.1021/acs.estlett.2c00187>.

- 895 (55) Yang, T.; Mai, J.; Wu, S.; Liu, C.; Tang, L.; Mo, Z.; Zhang, M.; Guo, L.; Liu, M.; Ma, J. UV/Chlorine  
896 Process for Degradation of Benzothiazole and Benzotriazole in Water: Efficiency, Mechanism and  
897 Toxicity Evaluation. *Sci. Total Environ.* **2021**, *760*, 144304.  
898 <https://doi.org/10.1016/j.scitotenv.2020.144304>.
- 899 (56) Malkin, Ya. N.; Kuzmin, V. A.; Pirogov, N. O. Primary Photochemical and Photophysical Processes in  
900 2,2,4-Trimethyl-2-Dii-hydroquinolines. *J. Photochem.* **1984**, *26* (2–3), 193–202.  
901 [https://doi.org/10.1016/0047-2670\(84\)80038-6](https://doi.org/10.1016/0047-2670(84)80038-6)